Available online at www.sciencedirect.com
SCIENCE DIRECT®
Journal of Nuclear Materials 340 (2005) 119–123
journal of nuclear materials
www.elsevier.com/locate/jnucmat

Letter to the Editors

Influence of annealing in air on transport properties of long-time oxidized layers of zirconium alloys

H. Frank *

Department of Solid State Engineering, Faculty of Nuclear Sciences and Physical Engineering, Czech Technical University, Trojanova 13, 120 00 Prague 2, Czech Republic

Received 16 July 2004; accepted 9 November 2004

Abstract

The change of resistivity and permittivity of oxide films grown 1554 days in water at 360 °C on tubes of Zr1Nb, ZrSnNb(Fe) and IMP Zry-4 was investigated by *I–V* measurements after long-time annealing in air at 123 °C. Thereby the room temperature resistivity, highest in Zry-4W and lowest in Zr1Nb, increased by more than two orders of magnitude due to a strong decrease of mobility, with nearly constant carrier concentration. The polarity of the zero current changed from negative to positive values in the pA range. The changes are thought to be due to continued oxidation.

1. Introduction

The results presented in this paper were achieved continuing the investigation of the transport properties of oxide layers of zirconium alloys described earlier [1]. Of special interest were three specimens [2] of oxide films on Zr1Nb, ZrSnNb(Fe) and IMP Zry-4 tubes, used for fuel cladding in light water reactors, which had been grown at VVER conditions in water of 360 °C for 1554 days ($4\frac{1}{4}$ years). The task was to compare the resistivity and the permittivity of the oxides grown under identical conditions on different alloys and test their stability at higher temperature by long-time annealing in air.

2. Experimental

Tube specimens 30 mm long and of 9 mm outer diameter prepared from the zirconium alloys Zr1Nb, ZrSnNb(Fe) and IMP Zry-4 (Table 1) had been oxidized in water at 360 °C for 1554 days ($4\frac{1}{4}$ years). Gold electrodes of about 200 nm thickness were vacuum evaporated on to the specimens wrapped in Al foil with circular openings of 6.0 mm diameter, and the samples were mounted in a mini-thermostat. The schematic measuring set-up was the same as used earlier [3].

Owing to the large contact area of 0.283 cm^2, guard rings appeared not to be necessary, as was shown already in [1]. The voltage was applied and measured at the zirconium metal. The gold electrode on the oxide layer was earthed via a picoampere-meter with a resolution of 0.1 pA. The voltage drop on the picoamperemeter was limited to 10 mV maximum. First the capacity was measured with a TESLA BM 498 type capcitance bridge, operating at 1000 Hz with 0.1% precision. Then the *I–V* characteristics were measured, first at room

* Tel.: +420 2 2435 8559; fax: +420 2 2191 2407/2243 58601.
E-mail address: frank@km1.fjfi.cvut.cz

0022-3115/$ - see front matter
doi:10.1016/j.jnucmat.2004.11.003

Table 1
Chemical composition (wt%) of zirconium alloys used in the present study

	Nb	Sn	Fe	Cr
Zr1Nb	1	–	–	–
ZrSnNb(Fe)	1	1	0.1	–
IMP Zry-4	–	1.3	0.2	0.1

temperature and then at constant higher temperatures between 60 and 120 °C with 20 °C steps. The voltage steps applied were 1, 2, 5, 10, 15, 20, 25, 30 V, respectively. The time dependence of the injection current was measured after each voltage increase, and reaching constant charge limited current conditions after 30 min, the time-dependent extraction short-circuit current drop was registered to evaluate the extracted charge, being equal to the injected charge. In order to assess the influence of oxygen on the properties of the oxide layers, the specimens were long-time annealed at 123 °C and the time dependence of the zero current was registered. The annealing was interrupted from time to time to measure the *I–V* characteristics at room temperature and trace the change of transport properties.

3. Results and discussion

The steady-state current at room temperature of the samples as grown as a function of the applied voltage is shown in Fig. 1. The *I–V* characteristics can be fitted to a second order polynomial

$$I = aU^2 + bU + c, \tag{1}$$

where c is the short-circuit current I_0 flowing at zero voltage. The linear term describes the current obeying Ohm's law, and $b = 1/R$ defines the resistance $R = \rho w/A$ of the sample with thickness w, contact area A and resistivity ρ. The quadratic term is due to the space-charge limited current according to the Mott-Guerney [4] relation

$$I = A\frac{9\varepsilon\varepsilon_0\mu}{8w^3}U^2. \tag{2}$$

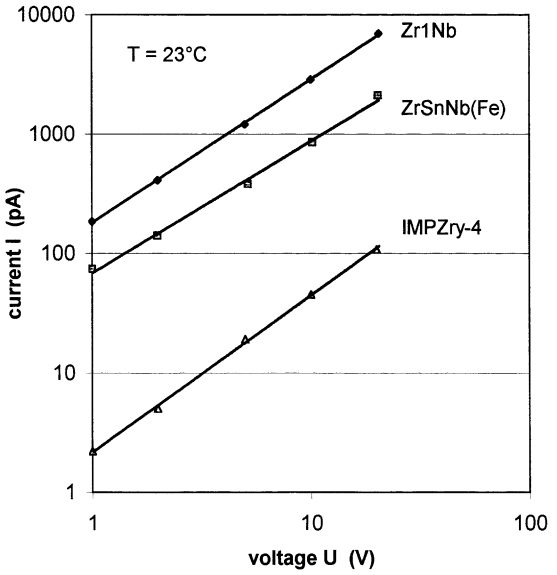

Fig. 1. *I–V* characteristics at room temperature, samples as-grown.

Using Eq. (2) it is possible to evaluate the mobility μ and the concentration n of the free carriers from the quadratic term in Eq. (1),

$$n = I/e\mu\rho. \tag{3}$$

The results of the measurements of the *I–V* characteristics at room temperature, using values from Fig. 1, are given in Table 2. It should be noted that the samples had been measured at room temperature and had not been exposed to higher temperatures. Although the oxides had been grown under the same conditions, there are large differences of their properties.

Measurements of the *I–V* characteristics at higher temperatures (starting from 60 °C with 20 °C increments up to 123 °C), allowed to evaluate the activation energy of resistivity, mobility and carrier concentration, shown in Table 3. It is interesting to note that the measurements at temperatures above room temperature changed appreciably the results, compared with Table 2. As can be seen in Table 3, the activation energy is higher for

Table 2
Transport parameters of the as-grown samples

			Zr1Nb	ZrSnNb(Fe)	IMP Zry-4w
Thickness	w	(μm)	27.1	35.9	37.5
Rel. permittivity	ε_r		24	28	18
Resistivity	ρ	(Ω cm)	4.3×10^{11}	1.3×10^{12}	4.5×10^{13}
Mobility	μ	(cm^2/Vs)	1.5×10^{-7}	1.1×10^{-9}	2.0×10^{-8}
Concentration	n	(cm^{-3})	1.0×10^{14}	4.4×10^{13}	7.0×10^{12}

Table 3
Activation energies of transport parameters

Samples		Zr1Nb	ZrSnNb(Fe)	IMP Zry-4
Activation energy of resistivity	(eV)	−0.64	−0.96	−1.07
Activation energy of mobility	(eV)	0.78	0.79	0.65
Activation energy of carrier concentration	(eV)	−0.14	0.14	−0.05

The sign of the activation energy indicates (+) increasing and (−) decreasing the parameter with rising temperature.

the samples with larger room temperature resistivity. In consequence of this, at 360 °C oxidation temperature, the resistivity of all three samples will be around $10^8\,\Omega\,\mathrm{cm}$. Owing to the lower activation energy of Zr1Nb, its resistivity will remain higher than that of the other samples, although the starting resistivity at room temperature was the lowest. This would explain the smaller thickness of the oxide film of Zr1Nb in comparison with the other zirconium alloys, if we assume [5] the oxidation velocity to be directly proportional to the conductivity of the oxide layer.

The mobility of the carriers is extremely low, about $10^{-7}\,\mathrm{cm^2/Vs}$ at room temperature, and nearly the same for all three zirconium alloys, but strongly increasing with rising temperature with not very different activation energies (0.65–0.79 eV). On the other hand, the carrier concentration is with $1\times10^{14}\,\mathrm{cm^{-3}}$ practically the same and furthermore, nearly temperature independent for all three zirconium alloys. The values of carrier concentration given in Table 2, which were computed from the measured *I–V* characteristics directly after contact evaporation, differ from the values assessed, when the samples had been at higher temperatures during measurement of the temperature dependence of resistivity. Already after the first measurements it could be seen that there existed a certain influence of past temperature, time and voltage treatment on further results. It was therefore decided to investigate the effect of prolonged impact of temperature and voltage.

The *I–V* characteristics at higher temperatures did not pass through zero, i.e. there existed a short-circuit current and an open-circuit voltage, similar to previous measurements on other samples. But on the contrary to former findings [1], the zero current was negative, and the open circuit voltage was positive (the polarity is related to the bulk zirconium). The short-time dependence of the injection and extraction currents is shown in Fig. 2.

Continued annealing at 123 °C resulted in a slow drop of the zero current with a final change to a positive and stabile zero current. The results are summarized in Table 4.

Thus the overall behaviour of injection and extraction currents is in principle the same for all three zirconium oxides. At application of a voltage, there flows an injection current (phase 1), which drops after about 1000 s to a space-charge limited steady current. At

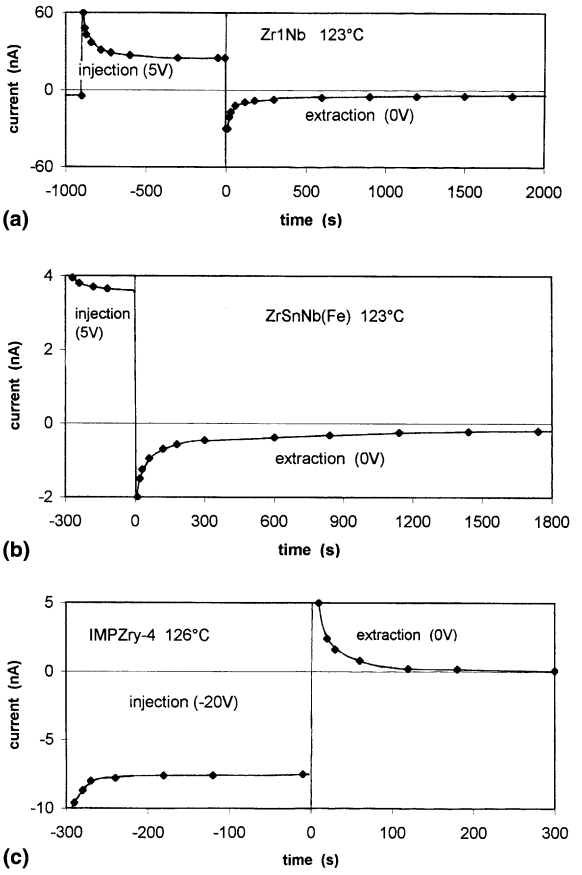

Fig. 2. Time dependence of injection and extraction currents (at 123 °C) (a) ZR1Nb (b) ZrSnNb(Fe), starting from negative zero current, injection at 5 V (c) IMP Zry-W, injection at −20 V.

shortening the sample by a pico-amperemeter, there flows an extraction current of opposite sign of the injection current (phase 2), which is the sign inverted replica of the injection current drop (Fig. 3), obeying a power law, $I_{\mathrm{extr}} = A\cdot t^{-n}$, (the exponent was $0.25 < n < 0.65$, rising with injection voltage and falling with temperature). The time-integral of the extraction current is equal to the injected charge, which is a linear function of the injection voltage.

From time to time the annealing was interrupted and the *I–V* characteristics were measured at room

Table 4
Injection and extraction currents at 123 °C

		Zr1Nb	ZrSnNb(Fe)	IMP Zry-4W
Stable injection current at voltage	(nA)	25	3.65	−7.5
	(V)	5	5	−20
Zero current after 1800 s	(pA)	−4500	−200	−60[a]
Time for change of polarity of zero current	(d)	5.4	0.46	5.8
Constant positive zero current after 14 days	(pA)	30	45	0.9

[a] Originally positive extraction current after 600 *s* changed to negative zero current.

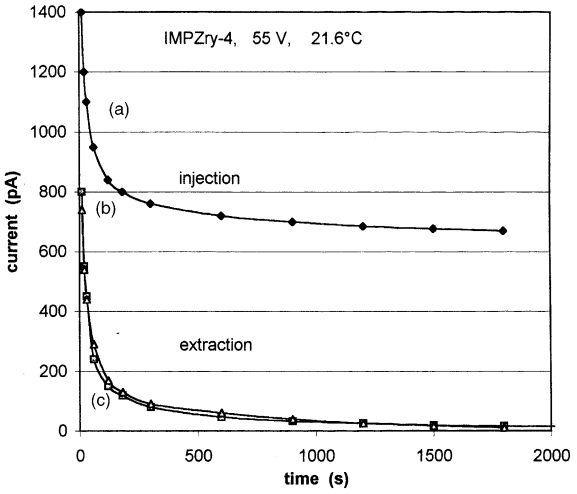

Fig. 3. The extraction current as the replica of the injection current. IMP Zry-4, measurement at room temperature before annealing, (a) time dependence of the current at application of 55 V, consisting of the time dependent injection current with added steady state current of 660 pA, (b) short circuit extraction current (of opposite polarity, here depicted positive), (c) current values of (a) after subtraction of 660 pA, being the pure injection current.

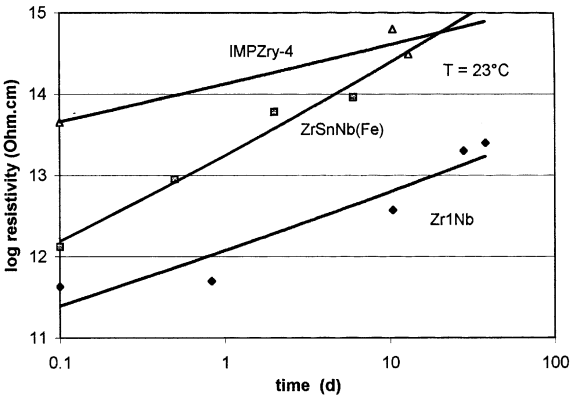

Fig. 4. Dependence of room temperature resistivity on time of annealing in air at 123 °C.

temperature. As can be seen in Fig. 4, the resistivity increased steadily with annealing time.

It is possible to compensate the zero current I_0 to zero by applying a voltage of opposite sign, which is equal to the open-circuit voltage U_0. Measurements of the zero current and of its compensation voltage represent a simple method of assessing the resistivity at a given temperature, because I_0 and U_0 constitute a small section of the linear part of the I–V characteristics at the origin.

4. Conclusions

Although all three samples had been grown under identical conditions, there are grave differences in their properties, see Tables 2–4. Zr1Nb is considered to be the best corrosion resistant material for fuel cladding. It had the smallest oxide layer thickness, and the permittivity had nearly the normal value of the compact oxide.

The negative zero current is caused by electrons, which had been injected as space charge by former positive injection currents, and are loosely bound to vacancies and are then thermally liberated. In case of the as-grown samples the origin of these electrons is not clear. The final positive zero current after long annealing is believed to be caused by the diffusion of oxygen from the surrounding air and chemically reacting with zirconium at the metal-oxide interface. At the annealing temperature oxygen diffuses through the oxide layer, thereby filling up vacant oxygen sites and thus increasing the distance between the remaining vacancies, which will strongly diminish the probability of electron hopping and thus lowering the mobility. It is not clear, why the concentration of current carriers is also not diminished, but slightly increases with annealing time.

Changes in the oxide structure by prolonged annealing in air are indicated by a change of the relative permittivity. It dropped from a starting value of 24 to 14 in Zr1Nb (−41%), from 28 to 24 in ZrSnNb(Fe) (−14%), and from 18.1 only a little to 17.5 in IMP Zry-4 (−3%). In the Zr1Nb sample the current $I_0 = 30$ pA transported a charge of 9.8×10^{-5} in 38 days as equaling $n = 6.2 \times 10^{14}$ electrons which, if used for oxidizing the Zr metal, would increase the oxide layer thickness only

by about 4×10^{-4} μm ($\Delta w = nW/(2\rho NA)$, where $W = 123.22$ is the molecular weight, $\rho = 5.56$ g/cm^3 the density, $N = 6.02 \times 10^{23}$ Avogadro's number and $A = 0.283$ cm^2 the contact area). The negligible thickness increase cannot explain the large permittivity changes.

It seems justifiable to assume that the large observed differences are due to the different alloying additives, as listed in Table 1.

Acknowledgment

Support of this work by ŠKODA ÚJP, Praha company, is highly appreciated. Special thanks are due to Ms Věra Vrtílková for providing the oxidized specimens of specified thickness.

References

[1] H. Frank, J. Nucl. Mater. 306 (2002) 85.
[2] V. Vrtílková, private communication.
[3] H. Frank, J. Nucl. Mater. 321 (2003) 115.
[4] N.F. Mott, R.W. Guerney, Electronic Processes in Ionic Crystals, Clarendon, Oxford, 1940.
[5] M.M.R. Howlader, K. Shiiyama, C. Kinoshita, M. Kutsuwada, M. Inagaki, J. Nucl. Mater. 253 (1998) 149.